

Spectroscopic and magnetic properties of three $M(\text{PO}_3)_3$ ($M = \text{Cr}$ and Mo) metaphosphates

José M. Rojo, José L. Mesa, Luis Lezama and Teófilo Rojo*

Departamento de Química Inorgánica, Facultad de Ciencias, Universidad del País Vasco, Apdo. 644, E-48080 Bilbao, Spain

Three metaphosphates with formula $M(\text{PO}_3)_3$ ($M = \text{Cr}$ and Mo) and $\text{Cr}_2(\text{P}_6\text{O}_{18})$ have been synthesized and characterized. IR data allow establishment of a good correlation between the vibrational frequencies and the chain or ring structures of the $M(\text{PO}_3)_3$ ($M = \text{Cr}, \text{Mo}$) metaphosphates and the $\text{Cr}_2(\text{P}_6\text{O}_{18})$ hexametaphosphate, respectively. The reflectance diffuse spectra show bands belonging to the Cr^{III} and Mo^{III} cations in octahedral symmetry. The values of $10Dq$ and Racah parameters B and C have been calculated. The percentage of reduction calculated for the B parameter ($\approx 70\%$) is indicative of a significant degree of covalence in the $M-\text{O}$ ($M = \text{Cr}, \text{Mo}$) bonds. The EPR spectra of the metaphosphate compounds have been explained on the basis of the existence of more than one different environment for the metallic cations. In doped aluminium metaphosphates with Cr^{III} and Mo^{III} ions the EPR data indicate the presence of one centre with $|D| > hv$ and two centres with $|D| < hv$. Magnetic measurements show an antiferromagnetic behaviour for all compounds. In the case of the $\text{Cr}_2(\text{P}_6\text{O}_{18})$ hexametaphosphate the existence of a weak ferromagnetism intrinsic to the sample has been observed at *ca.* 3 K.

The study of phosphates of transition elements with low oxidation states has received great interest in recent years. These compounds exhibit interesting properties such as magnetic, heterogeneous catalysis, ionic exchange, *etc.*, with potential applications.^{1,2} In this way, the $M(\text{PO}_3)_3$ materials are interesting owing to the activity of Cr-containing aluminophosphates (CrAPO-5 materials) which are well known for their catalytic performances.^{3,4} The great ability of the phosphate frameworks to stabilize reduced oxidation states is a consequence of the relatively high charge in the PO_4^{3-} tetrahedra that favours the formation of anionic frameworks with a high degree of mechanical, chemical and thermal stability. For the molybdenum system, different synthetic methods to prepare new phases have been described.¹ Unfortunately, even if good crystals for X-ray structure determination were obtained, pure phases have not been prepared. This fact has precluded carrying out any study on the physical properties of these materials. Recently, a method based on the control of Mo/P ratio in the reaction medium has allowed the synthesis of pure phases with different oxidation states.⁵

The $M(\text{PO}_3)_3$ ($M = \text{Al}, \text{Sc}, \text{Ti}, \text{V}, \text{Mo}, \dots$) metaphosphates are the most condensed phosphate systems where the metal ions present unusual oxidation states.⁶⁻¹¹ For the $\text{Mo}(\text{PO}_3)_3$ compound only one phase has been isolated^{5,12} the structure of which has recently been reported.¹¹ In the chromium metaphosphates, six different polymorph phases have been described^{13,14} but the crystal structures of only two phases are known.^{15,16} One of them is shown to be isostructural with the molybdenum phase. For these compounds, the crystal structure may be described as formed by isolated MO_6 octahedra linked through infinite $[\text{PO}_3]_\infty$ chains of PO_4 tetrahedra [Fig. 1(a)].⁶⁻¹¹ Each MO_6 group is bridged to six neighbouring MO_6 octahedra by phosphate groups and each octahedron shares its six apices with six different PO_4 tetrahedra. These tetrahedra lie in adjacent layers and lead to a three-dimensional network, in which the metallic cations occupy three different crystallographic positions for the molybdenum compound. For the chromium metaphosphate Yakubovich *et al.*¹⁵ proposed the existence of only one crystallographic position for the Cr^{III} cations considering a subcell ($b/3$). As was observed, the structures of these phases show a superlattice effect in the b direction, based upon a $b/3$ subcell. The reason for the subcell effect is not immediately apparent in this complex structure.

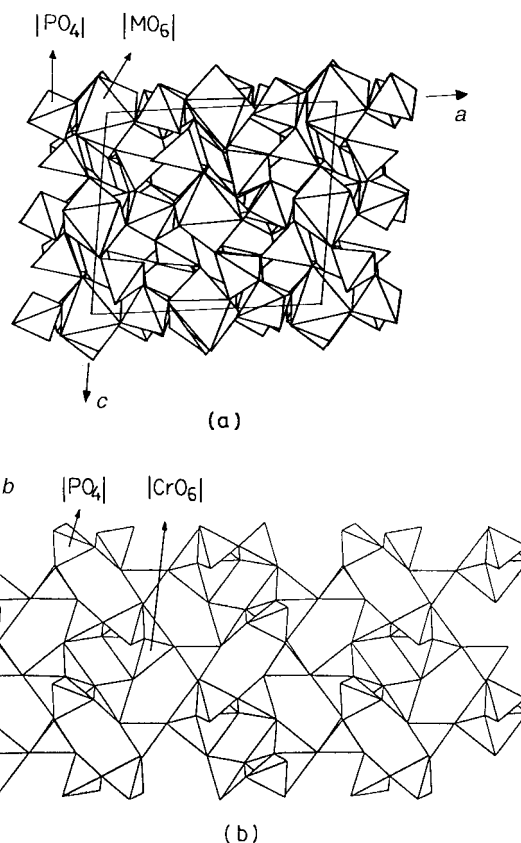


Fig. 1 Crystal structures of (a) $M(\text{PO}_3)_3$ ($M = \text{Cr}, \text{Mo}$) and (b) $\text{Cr}_2(\text{P}_6\text{O}_{18})$

It is necessary to perform a symmetry analysis to elucidate any translational pseudosymmetry that may occur *via* concerted polyhedral rotations.⁸

The crystal structure for the other chromium phase, namely the hexametaphosphate, is formed by CrO_6 octahedra linked through PO_4 tetrahedra belonging to $\text{P}_6\text{O}_{18}^{6-}$ cycles, [Fig. 1(b)]. The CrO_6 coordination polyhedra are not vertex- or edge-shared, and are isolated by PO_4 tetrahedra. Each

CrO₆ octahedron interacts with four P₆O₁₈⁶⁻ cycles, three phosphorus atoms lie in the plane defined by the Cr^{III} ion and the other three are placed below and above of the metallic cation in a perpendicular plane, leading to a three-dimensional network.¹⁶

In this work we present the study of the spectroscopic and magnetic properties of three metaphosphates, two of chromium (compounds **1** and **2**) and the other of molybdenum (**3**).

Experimental

Synthesis of the compounds

The M(PO₃)₃ (M=Cr **1** and Mo **3**) phases were prepared starting with a mixture of CrO₃ or MoO₃ and (NH₄)₂HPO₄, with a molar ratio of 1M:10P. The mixture was placed in an alumina crucible, heated at 250 °C for 4 h and heated to 800 °C. Clear green and yellow samples were obtained for the chromium and molybdenum phases, respectively. Compound **2** was prepared under the same conditions, but using a Cr/P ratio of 1:5; this phase is dark green. Attempts to attain a similar phase to that obtained for the molybdenum compound was not successful. The obtained compounds were washed with water and dried over P₂O₅ for 24 h. The metal ions and phosphorus contents were confirmed by ICP analysis. Found: Cr, 17.8; P, 31.8. Cr(PO₃)₃ **1** requires Cr, 18.0; P, 32.2. Mo, 28.4; P, 27.7. Mo(PO₃)₃ **3** requires: Mo, 28.8; P, 27.9. Cr, 17.7; P, 31.9. Cr₂(P₆O₁₈) **2** requires: Cr, 18.0; P, 32.2%.

X-Ray crystallography

A STOE automatic powder diffraction system, operating at 40 kV, 20 mA, with monochromatic Cu-Kα₁ radiation (1.5406 Å), was used to record the X-ray powder diffraction patterns of all compounds. A ω-2θ scan was performed, with steps of 0.05° in 2θ, and a fixed-time counting of 5 s. The LSUCRE program¹⁷ was used to study the X-ray powder diffraction patterns of the compounds.

Physicochemical characterization techniques

IR spectra (KBr pellets) were obtained with a Nicolet FT-IR 740 spectrophotometer. Diffuse reflectance spectra were registered at room temperature on a Cary 2415 spectrometer in the range 8000–50 000 cm⁻¹. A Bruker ESP 300 spectrometer, operating at X and Q bands, was used to record the EPR polycrystalline spectra between 4.2 and 300 K. The temperature was stabilized by an Oxford Instrument (ITC 4) regulator. The magnetic field was measured with a Bruker BNM 200 gaussmeter and the frequency inside the cavity was determined using a Hewlett-Packard 5352B microwave frequency counter. Magnetic measurements were performed on polycrystalline samples between 1.8 and 300 K, using a Quantum Design SQUID magnetometer (MPMS-7) with a magnetic field of 0.1 T at which the magnetization *vs.* magnetic field is linear even at 1.8 K.

Results and Discussion

The X-ray powder diffraction patterns of both compounds **1** and **3** have been indexed using the LSUCRE program¹⁷ in a monoclinic unit cell with space group *Ic*, previously determined by Watson *et al.*¹¹ from single-crystal X-ray data (Table 1). From this Table, it can be seen that the unit-cell dimensions obtained for compounds **1** and **3** are similar, and correspond to two cations, chromium and molybdenum, belonging to the first and second series of transition metals, respectively. Moreover, the X-ray powder diffraction pattern of the chromium metaphosphate can also be indexed in the *b*/3 subcell given by Yakubovich *et al.*,¹⁵ see Table 1.

In compound **1**, the study of the powder diffraction data

does not permit deduction of the unmistakable presence of chromium ions in one or three different crystallographic positions. The indexing of the X-ray powder diffraction pattern for compound **2** was carried out by using the LSUCRE program¹⁷ in a monoclinic cell with space group *P2₁/a*. In this case, only one position can be confirmed for the chromium ions as described by the single-crystal data.¹⁶ The calculated densities for these compounds are in agreement with the measured values obtained by the hydrostatic method (Table 1).

IR spectroscopy

Different types of phosphates with a definite structural type (ortho, pyro, chain or ring structure) can be identified by IR spectroscopy.^{18,19} Metaphosphate compounds are classified in two large families of chain and ring structures. For these condensed phosphates, an approximation may be needed due to the existence of two types of P–O bonds: for an 'external' oxygen, the P–O_{ext} distance is shorter (and the stretching frequency accordingly higher) than for an 'internal' (or bridging) oxygen within the P–O–P chain or ring. Moreover, in short-chain polyphosphates, a further splitting takes place owing to the existence of PO₂ and PO₃ groups in the anions. The common features of all metaphosphates are the existence in the PO₂ groups of P–O_{ext} distances shorter than those observed in the PO₃ and PO₄ groups of diphosphate and phosphate compounds, respectively.^{19,20} In this way, the most characteristic feature of a metaphosphate compound (whatever its chain or ring structure) is the existence of one or several strong IR bands at frequencies > 1200 cm⁻¹.

Selected IR bands of **1–3** are shown and compared with other isomorphous metaphosphates in Table 2. Band assignments have been empirically made on the basis of other metaphosphates given in the literature.^{18,19} The strong band observed at *ca.* 1250 cm⁻¹ can be attributed to the P–O_{ext} antisymmetric stretching vibrations of the metaphosphate groups. Additional bands of variable intensity are also observed in the range 1200–1010 cm⁻¹. These bands are also due to P–O_{ext} vibrations with mixed symmetric–antisymmetric properties. The band attributed to ν_{as}(P–O_{int}) for the metaphosphates with chain structure appears in the range 950–980 cm⁻¹. For compound **2** this band appears shifted to higher frequencies as an intense doublet at *ca.* 1000 cm⁻¹,^{19,21} which is characteristic of metaphosphates exhibiting a ring structure (cyclophosphates P₃O₆).

However, the region with more precise information concerning the structural characterization corresponds to the symmetric P–O–P stretching vibrations. Metaphosphates **1** and **3**, which exhibit chain structures, show at least four signals of medium intensity centred at 775, 760, 725 and 685 cm⁻¹ and 775, 745, 705 and 675 cm⁻¹, respectively. In compound **2** the intense ν_s(P–O_{int}) vibration corresponding to the cyclophosphate (P₃O₆) is observed at 790 cm⁻¹, close to that observed for low-symmetry compounds in which this signal appears in a narrow range (780–765 cm⁻¹).^{19,22} Consequently, considering both the existence of four signals and the low frequency at which those bands appear a chain structure for compounds **1** and **3** can be confirmed.

Finally, bands with poor resolution appear at 610 and 440 cm⁻¹. These bands can be assigned to the antisymmetric stretching modes in the MO₆ octahedra [ν_{as}(M–O)], probably coupled with the antisymmetric bending modes of the chain and cyclophosphate groups [δ_{as}(O–P–O)].^{23–25}

UV–VIS spectroscopy

The diffuse reflectance spectra were registered in the range 8000–50 000 cm⁻¹ and bands are listed in Table 3. Two strong absorptions were observed at 16 000, 22 500 and 15 800, 22 000 cm⁻¹ for the chromium compounds **1** and **2**, respectively. The bands corresponding to the molybdenum meta-

Table 1 Unit-cell dimensions of $M(\text{PO}_3)_3$ ($M=\text{Cr } 1, \text{Mo } 3$) and $\text{Cr}_2(\text{P}_6\text{O}_{18}) 2$

compound	$a/\text{\AA}$	$b/\text{\AA}$	$c/\text{\AA}$	$\beta/^\circ$	$V/\text{\AA}^3$	Z	$\rho_{\text{exp}}/\text{g cm}^{-3}$	$\rho_{\text{calc}}/\text{g cm}^{-3}$
$\text{Cr}(\text{PO}_3)_3$ 1	10.5276(6)	19.029(1)	9.3431(5)	98.126(3)	1852.9(4)	12	3.11	3.12 ^a
— ^b	10.5141(5)	6.3147(3)	9.3317(5)	98.126(3)	613.3(1)	4		
$\text{Mo}(\text{PO}_3)_3$ 3	10.8033(2)	19.4855(4)	9.5933(2)	97.769(2)	2000.9(1)	12	3.27	3.29 ^c
$\text{Cr}_2(\text{P}_6\text{O}_{18})$ 2	8.319(3)	15.228(6)	6.225(2)	105.85(2)	758.7(6)	2	2.51	2.54 ^d

^aRef. 14; ^bref. 15; ^cref. 12; ^dref. 16.

Table 2 Selected IR bands (cm^{-1}) and empirical assignments for several $M(\text{PO}_3)_3$ metaphosphates, $M=\text{Al}, \text{Sc}, \text{Cr } 1, \text{Mo } 3$ and one hexametaphosphate $\text{Cr}_2(\text{P}_6\text{O}_{18})$ **2**, between 400 and 1500 cm^{-1} ^a

assignment	Al	Sc	Cr 1	Mo 3	Cr 2
$\nu_{\text{as}}(\text{P}-\text{O}_{\text{ext}}) \text{PO}_2$	1275vs 1200s 1185s 1145s	1265vs 1200s 1180s 1125s	1240vs 1160s 1130s	1250vs 1125s 1085s	1255vs 1175s 1155s 1080s
$\nu_{\text{s}}(\text{P}-\text{O}_{\text{ext}}) \text{PO}_2$			1095vs		
$\nu(\text{P}-\text{O}_{\text{ext}}) \text{PO}_3$	1040s 1020s	1045s	1050s 1020s	1025s 1010s	
$\nu_{\text{as}}(\text{P}-\text{O}_{\text{int}}) \text{P}-\text{O}-\text{P}$	965s 780m 725m	970s 770m 755m	975s 775m 760w	955s 775m 745m	1000s 975s 790s
$\nu_{\text{s}}(\text{P}-\text{O}_{\text{int}}) \text{P}-\text{O}-\text{P}$	710m	715m	725m	705m 675m	
$\nu_{\text{as}}(\text{M}-\text{O})$	680w 610w	680m 610m	685w 570m 560m	610w	585m 560m
$\delta_{\text{as}}(\text{O}-\text{P}-\text{O})$	550m 530m 490s 475s	540m 510m 440m	520m 490m	545m 500s 470m	535m 500m 485 m

^avs = very strong, s = strong, m = medium, w = weak.

Table 3 Diffuse reflectance data of $M(\text{PO}_3)_3$ ($M=\text{Cr } 1, \text{Mo } 3$) and $\text{Cr}_2(\text{P}_6\text{O}_{18})$ **2**

	Cr 1		Mo 3		Cr 2	
	E/cm^{-1}	E/B	E/cm^{-1}	E/B	E/cm^{-1}	E/B
${}^4\text{A}_{2g} \rightarrow {}^4\text{T}_{2g}(\text{F})$	16000	22.1	23000	50.3	15800	25.5
${}^4\text{A}_{2g} \rightarrow {}^4\text{T}_{1g}(\text{F})$	22500	34.6	28100	61.5	22000	35.5
${}^4\text{A}_{2g} \rightarrow {}^2\text{E}_g$	14700	20.3	10200	22.3	14600	23.5
${}^4\text{A}_{2g} \rightarrow {}^2\text{T}_{1g}$	15400	21.3	10600	23.2	15300	24.5
${}^4\text{A}_{2g} \rightarrow {}^2\text{T}_{2g}$	21300	29.4	16000	35.0	21800	35.0
Dq/cm^{-1}	1600		2300		1580	
B/cm^{-1}	650		457		620	
C/cm^{-1}	3390		2180		3412	
% reduction	71		75		68	

phosphate (compound **3**) were observed at 23 000 and $28\,100 \text{ cm}^{-1}$. The results are in good agreement with those observed for the Cr^{III} and Mo^{III} compounds in octahedral symmetry.^{26–30}

Using a simple crystal-field approximate model, the ligand-field splitting parameter $10Dq$ and the Racah parameter B may be calculated from the energies of the two lower spin-allowed transitions. For $\text{Cr}(\text{PO}_3)_3$ **1** we find $Dq=1600 \text{ cm}^{-1}$ and $B=650 \text{ cm}^{-1}$, and for $\text{Mo}(\text{PO}_3)_3$ **3** $Dq=2300 \text{ cm}^{-1}$ and $B=457 \text{ cm}^{-1}$. The values obtained for compound **2** are 1580 and 620 cm^{-1} for the Dq and B parameters, respectively. These values are close to those reported for other Cr^{III} and Mo^{III} compounds.^{26–31} The B values for **1–3** are approximately 70% of those corresponding to the free ions (918 and 610 cm^{-1} for the chromium and molybdenum ions, respectively). This fact

implies a significant degree of covalence in the $\text{M}-\text{O}$ ($M=\text{Cr}, \text{Mo}$) bonds.

The weak absorptions observed at 14 700, 15 400 and 14 600, $15\,300 \text{ cm}^{-1}$ for compounds **1** and **2** respectively, and 10 200 and $10\,600 \text{ cm}^{-1}$ for compound **3**, may be assigned to the spin-forbidden transitions ${}^4\text{A}_{2g} \rightarrow {}^2\text{E}_g$, ${}^2\text{T}_{1g}$ considering the ratios Dq/B of 2.46 and 2.55 and 5.03 for the chromium and molybdenum phases. The signals of lower energy can be attributed to the transition ${}^4\text{A}_{2g} \rightarrow {}^2\text{E}_g$ given in the diagram levels of Fig. 2. The values of the C parameters obtained from the forbidden transitions are 3390, 3412 and 2180 cm^{-1} , respectively. Finally, the weak absorptions observed at 21 300, 21 800 and $16\,000 \text{ cm}^{-1}$ for compounds **1**, **2** and **3** respectively, may be assigned to the spin-forbidden transition ${}^4\text{A}_{2g} \rightarrow {}^2\text{T}_{2g}$. In the case of the molybdenum metaphosphate this band appears at

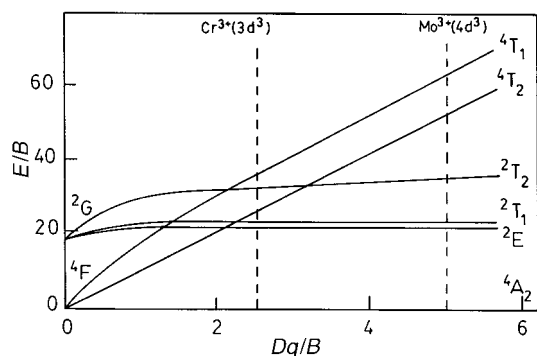


Fig. 2 Energy-level diagram for the d^3 configuration in an octahedral field

lower frequency than that observed for the spin-allowed transition ${}^4A_{2g} \rightarrow {}^4T_{2g}(F)$ as expected following the energy levels of these compounds (Fig. 2).

The diffuse reflectance data show that both allowed and forbidden transitions have higher E/B ratios in the molybdenum metaphosphate than in the chromium phases. This fact is due to the different positions of the metallic ions in the transition series (Table 3). Besides, the value of the Racah parameter B is higher in the chromium compounds than in the molybdenum phase, but the percentage of reduction of the B parameter ($\approx 70\%$) is indicative of a similar degree of covalence in the $M-O$ ($M=Cr, Mo$) bonds, in these compounds.

EPR Spectroscopy

The EPR spectra of the title compounds at 4.2 K are given in Fig. 3. For the $Mo(PO_3)_3$ phase no signal was observed at temperatures higher than 120 K. Therefore, we can attribute the signal observed at low temperatures to the Mo^{III} ions present in the compound and enable us to exclude the existence of Mo^V impurities.^{32,33} The spectrum can only be explained by considering the presence of more than one different environment for molybdenum in this compound (Fig. 3). Assuming that the g tensors are isotropic, as usually occurs for Mo^{III} compounds, an average g value of 1.89 can be deduced. The intensity of the signal was so weak that the spectrum at Q-band cannot be recorded. In the case of the chromium phases, the EPR spectra show isotropic signals with $g = 1.97$ (Fig. 3). The linewidth for the $Cr_2(P_6O_{18})$ compound is larger than that observed for the $Cr(PO_3)_3$ phase. This result is indicative

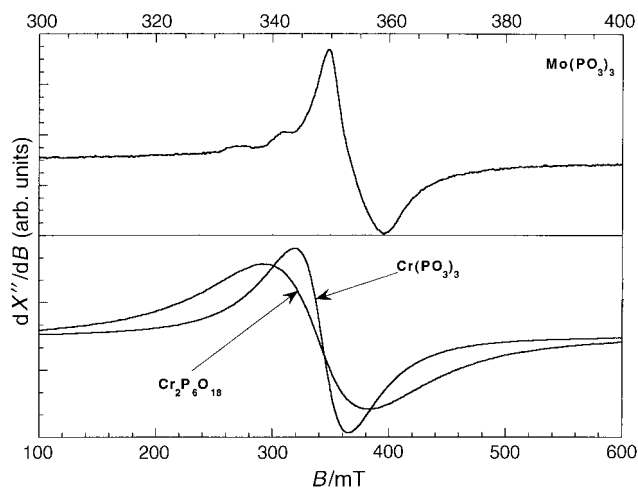


Fig. 3 EPR spectra of $Mo(PO_3)_3$, $Cr(PO_3)_3$ and $Cr_2(P_6O_{18})$ recorded at 4.2 K

of the important role of the magnetic exchange interactions in the latter phase.

In order to obtain more information about the local symmetry of the M^{III} centres, EPR spectra were measured on molybdenum- and chromium-doped phases of the homologous aluminium metaphosphates between 4.2 and 300 K. In the case of the Mo^{III} compounds the best resolution was obtained for $Al(PO_3)_3:0.1\%Mo$ (Fig. 4). The central g value is 1.91. Effects of the zero-field splitting of the $S=3/2$ ground state are observed but it is not possible to obtain quantitative information of the structure in the spectrum. However, the signals observed between 320 and 380 mT are indicative of at least two different Mo^{III} sites with D values $< 0.1 \text{ cm}^{-1}$. A new signal, centred at *ca.* 180 mT, appears at temperatures lower than 30 K (see the inset of Fig. 4). This signal with $g_{eff} \approx 4$ could be attributed to another metallic centre for which $|D| \gg hv$.³³

All the attempts to prepare the aluminium hexametaphosphate phases doped with chromium were unsuccessful. The obtained compounds were the metaphosphate phases. In the case of the chromium metaphosphate the best EPR resolution was obtained for $Al(PO_3)_3:2\%Cr$ (Fig. 5). Lower concentrations of chromium give rise to new signals from a non-identified phase. In spite of the analogies between the Cr^{III} and Mo^{III} ions, the spectrum for the chromium phase is different from that obtained for $Al(PO_3)_3:0.1\%Mo$. The X- and Q-

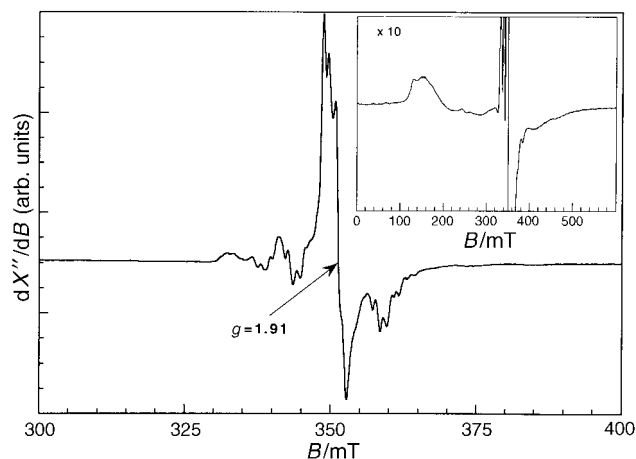


Fig. 4 EPR spectrum of $Al(PO_3)_3:0.1\%Mo$ at 4.2 K. Inset shows the signal corresponding to $g_{eff} \approx 4$.

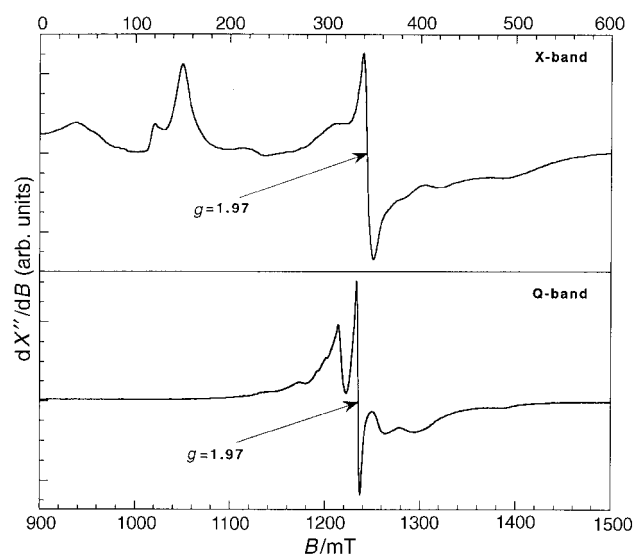


Fig. 5 X- and Q-band EPR spectra of $Al(PO_3)_3:2\%Cr$, registered at 4.2 and 100 K, respectively

band spectra (Fig. 5) show that the observed splittings are nearly frequency independent and this can be attributed to the zero-field splitting of the Cr^{III} ion. In the X-band spectrum, the most characteristic signals are observed at *ca.* 350, 175 mT and near zero-field. We have not carried out any simulation of the EPR spectra of these multiple chromium(III) phases. However, considering the simulations reported by other authors^{3,34,35} the observed EPR spectra may suggest the presence of three different sites for the chromium ions in the Cr(PO₃)₃ phase. One of them with $|D| > h\nu$ and the other two with $|D| < h\nu$. These results are in good agreement with the crystallographic data that show the existence of an octahedron with a larger distortion than that observed for the other two.

Magnetic properties

The thermal evolution of the molar magnetic susceptibility for Mo(PO₃)₃ is shown in Fig. 6. A sharp maximum is observed at 4.5 K, indicating the existence of an antiferromagnetic ordering in this compound. The high-temperature data ($T > 50$ K) are well described by a Curie–Weiss law [$\chi = C_m/(T - \theta)$] with $C_m = 1.71 \text{ cm}^3 \text{ K mol}^{-1}$ and $\theta = -6.8$ K. The negative temperature intercept together with the decrease of the effective magnetic moment observed when the temperature is lowered ($3.64 \mu_B$ at 300 K and $1.78 \mu_B$ at 2 K) are in good agreement with the predominance of antiferromagnetic interactions in this compound (Fig. 6).

Considering the structural features of the molybdenum metaphosphate only superexchange interactions *via* PO₄ tetrahedra can be expected. Due to the complexity of the three-dimensional arrangement and the consequent presence of different exchange pathways it is not possible to find a simple magnetic model, representing exactly the characteristics of the magnetic ordering in this compound. However, taking into account the weakness of the exchange couplings and the packing of the MoO₆ octahedra, a simple cubic network can be utilised in order to obtain an approximate value of the exchange parameter. Considering the usual isotropic magnetic behaviour of Mo^{III} ions a Heisenberg hamiltonian was the starting point:

$$H = -2J \sum_{i < j} S_i S_j$$

and using the high-temperature series expansion developed by Rushbrooke and Wood³⁶ the following analytical expression for the magnetic susceptibility is deduced for a Heisenberg simple cubic antiferromagnetic system with $S = 3/2$:

$$\chi_m = \frac{5 Ng^2 \beta^2}{4 kT} \left(1 + \frac{15}{x} + \frac{45}{x^2} + \frac{64}{x^3} + \frac{844.375}{x^4} + \frac{3485.775}{x^5} + \frac{48638.9}{x^6} \right)^{-1}$$

where $x = kT/J$

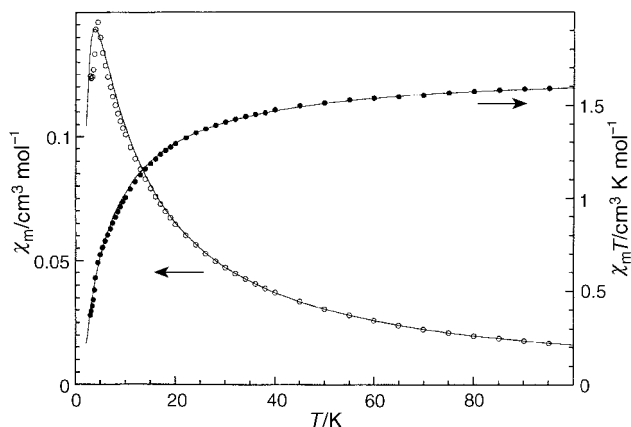


Fig. 6 Thermal variation of χ_m and $\chi_m T$ for Mo(PO₃)₃

The best fit of the experimental data to the above equation was obtained for $g = 1.90$ and $J/k = -0.38$ K, and it is represented by the solid line in Fig. 6. In spite of the differences between the real system and the employed model, the calculated curve follows quite well the experimental data. Moreover, taking into account that the knowledge of only six terms of the infinite series are valid for the equation used when T decreases to near T_N it can be concluded that the molybdenum metaphosphate is well described as a three-dimensional Heisenberg antiferromagnet with a J/k value of *ca.* 0.4 K.

The magnetic behaviour of Cr(PO₃)₃ is very similar to that exhibited by the homologous molybdenum compound. The susceptibility *vs.* temperature curve shows a maximum at 4.5 K (Fig. 7), obeying the Curie–Weiss law with $C_m = 1.83 \text{ cm}^3 \text{ K mol}^{-1}$ and $\theta = -2.7$ K. Considering the analogies between both compounds, from the structural and electronic point of view, this result is not surprising. The most important difference is observed for the Curie constant, which exhibits higher values for the chromium than for the molybdenum compound. This fact results from the effect of the spin–orbit coupling which is less important for an element of the first transition series such as chromium. Consequently, a lower deviation from the free-electron g value and a higher C_m value are observed in this case. A simple treatment as was described above for the molybdenum metaphosphate allows us to conclude that the Cr(PO₃)₃ phase orders as a three-dimensional Heisenberg antiferromagnet with a J/k value of *ca.* 0.3 K.

The magnetic behaviour of the Cr₂(P₆O₁₈) hexametaphosphate is substantially different from that observed for the chromium metaphosphate. The χ_m *vs.* T curve does not exhibit any appreciable anomaly at applied magnetic fields > 1 T (Fig. 7). The high-temperature data follow a Curie–Weiss law with $C_m = 1.83 \text{ cm}^3 \text{ K mol}^{-1}$ and $\theta = -0.2$ K. The value of the Curie constant is practically the same as that observed for Cr(PO₃)₃. This result is in good agreement with the similar environment observed for the Cr^{III} ions and the negligible influence of the magnetic interactions above 50 K for both compounds. The magnetic effective moment measured under an applied magnetic field of 0.1 T decreases from $3.82 \mu_B$ at room temperature to $3.09 \mu_B$ at 1.8 K, showing the existence of antiferromagnetic interactions in the compound. χ_m as a function of temperature at lower applied magnetic fields rises below *ca.* 3 K indicating a magnetic transition (inset in Fig. 7). A very sharp peak in $-d(\chi T)/dT$ *vs.* T provides a more accurate ordering temperature of $T_N = 2.2$ K. Magnetization as a function of applied field at below and above T_N is shown in Fig. 8. The linear increase of the magnetization above 0.1 T and the absence of saturation behaviour up to 7 T imply an antiferromagnetic-like ordering. However the magnetization data at low applied fields, as shown in Fig. 8, indicate a small amount of a ferromagnetic

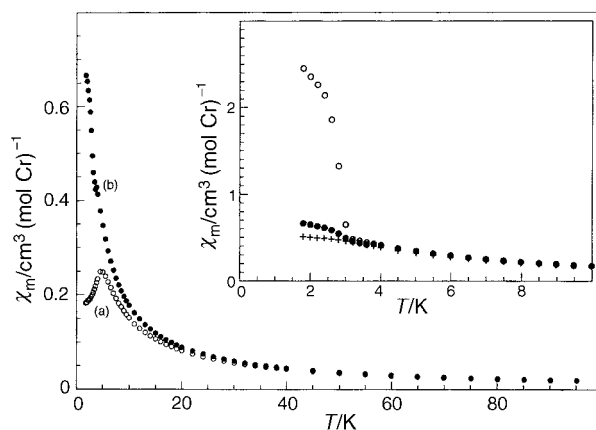


Fig. 7 Thermal variation of χ_m for Cr(PO₃)₃ [(a), ○] and Cr₂(P₆O₁₈) [(b), ●]. Inset shows the thermal evolution of χ_m for the Cr₂(P₆O₁₈) compound at different magnetic fields (○, 10 mT; ●, 100 mT; +, 1 T).

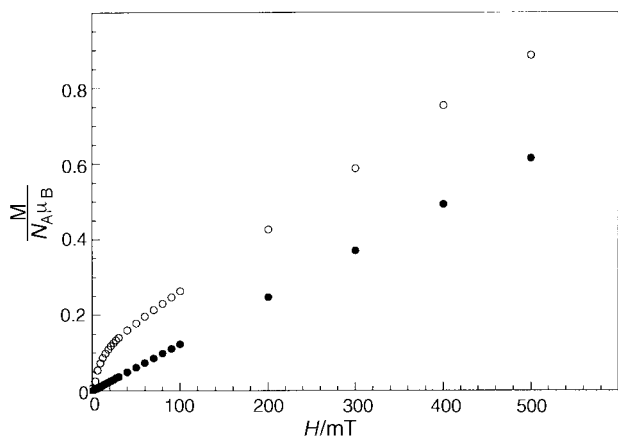


Fig. 8 Magnetization vs. applied magnetic field, below (○) and above (●) T_N for the $\text{Cr}_2(\text{P}_6\text{O}_{18})$ compound

component in the ordered state that appears to be responsible for the steep increase in χ_m at the ordering temperature. This magnetic behaviour is consistent with the existence of a weak ferromagnetism intrinsic to the sample. To understand the magnetic structure in the ordered state, neutron diffraction studies above and below T_N would be necessary.

Conclusion

The $\text{M}(\text{PO}_3)_3$ ($\text{M}=\text{Cr}$ and Mo) metaphosphates and $\text{Cr}_2(\text{P}_6\text{O}_{18})$ hexametaphosphate have been synthesized and studied by using X-ray diffraction, spectroscopic and magnetic techniques. The IR data of the metaphosphate compounds exhibit four bands corresponding to the $\nu_s(\text{P}-\text{O}_{\text{int}})$ vibrations which confirm a chain structure for these phases. In the case of the chromium hexametaphosphate only one intense band appears in this region which is consistent with a ring structure in this compound. The bands observed in the diffuse reflectance spectra confirm that the Cr^{III} and Mo^{III} cations are placed in environments with an approximately octahedral symmetry. The $10Dq$ and Racah parameters have been calculated from the energy of these bands. The E/B ratios for both the allowed and forbidden transitions in the molybdenum metaphosphate are higher than those obtained for the chromium compounds in good agreement with their positions in the transition series. The EPR spectra of the title compounds at room temperature exhibit isotropic signals with g values of 1.89 and 1.98 for the molybdenum and chromium phases, respectively. For $\text{Cr}_2(\text{P}_6\text{O}_{18})$ the linewidth is larger than that observed for the chromium metaphosphate in accordance with the different magnetic exchange interactions present in both phases. The EPR spectra of the doped metaphosphates show the presence of three different sites with $|D| > \hbar\nu$ for one centre and $|D| < \hbar\nu$ for the other two. For $\text{Al}(\text{PO}_3)_3:0.1\%\text{Mo}$ the presence of a signal, $g_{\text{eff}} \approx 4$, observed at temperatures lower than 30 K has been attributed to the existence of a metallic centre corresponding to a D value of $|D| \gg \hbar\nu$. Magnetic measurements show a similar antiferromagnetic behaviour for both $\text{M}(\text{PO}_3)_3$ ($\text{M}=\text{Cr}, \text{Mo}$) metaphosphates. The J/k exchange parameters have been calculated by fitting the experimental magnetic data to a simple Heisenberg cubic antiferromagnetic model. Similar values of J/k (-0.30 and -0.40 K) have been obtained for both chromium and molybdenum metaphosphates. The magnetic study of the hexametaphosphate compound shows the existence of antiferromagnetic interactions. The presence of a

weak ferromagnetism, probably due to a misalignment of spins between different sublattices not exactly antiparallel, was observed at *ca.* 3 K. Magnetic interactions in these compounds are propagated by different exchange pathways *via* PO_4 tetrahedra.

This work was financially supported by the Government of the Basque Country (grant PGV PI-9439), which we gratefully acknowledge.

References

- 1 R. C. Haushalter and L. A. Mundi, *Chem. Mater.*, 1992, **4**, 31.
- 2 A. Clearfield, *Chem. Rev.*, 1988, **88**, 125.
- 3 B. M. Weckhuysen, R. A. Schoonheydt, F. E. Mabbs and D. Collison, *J. Chem. Soc., Faraday Trans.*, 1996, **92**, 2431.
- 4 J. D. Chen, J. Dakka, E. Neeleman and R. A. Sheldon, *J. Chem. Soc., Chem. Commun.*, 1993, 1379.
- 5 L. Lezama, J. M. Rojo, J. L. Pizarro, M. I. Arriortua and T. Rojo, *Solid State Ionics*, 1993, **63–65**, 657.
- 6 H. Van der Meer, *Acta Crystallogr., Sect. B*, 1976, **32**, 2423.
- 7 A. I. Domanskii, Yu. F. Shepelev, Yu. I. Smolin and B. N. Litvin, *Sov. Phys. Crystallogr.*, 1982, **27**, 140.
- 8 W. T. A. Harrison, T. E. Gier and G. D. Stucky, *Acta Crystallogr., Sect. C*, 1994, **50**, 1643.
- 9 P. Rittner and R. Glaum, *Z. Kristallogr.*, 1994, **209**, 162.
- 10 N. Middlemiss, F. Hawthorne and C. Calvo, *Can. J. Chem.*, 1977, **55**, 1673.
- 11 I. M. Watson, M. M. Borel, J. Chardon and A. Leclaire, *J. Solid State Chem.*, 1994, **111**, 253.
- 12 R. M. Douglass and E. Staritzky, *Anal. Chem.*, 1957, **29**, 985.
- 13 P. Remy and A. Boullé, *C. R. Acad. Sci. Paris*, 1964, **258**, 927.
- 14 P. Remy and A. Boullé, *Bull. Soc. Chim. Fr.*, 1972, **6**, 2213.
- 15 O. V. Yakubovich, O. V. Dimitrova and G. V. Savina, *Kristallografiya*, 1991, **34**, 486.
- 16 M. Bagieu-Beucher and J. C. Guitel, *Acta Crystallogr., Sect. B*, 1977, **33**, 2529.
- 17 D. E. Appleman and K. T. Evans, *Indexing and Least-Squares Refinement of Powder Diffraction Data*, N.T.I.S. Document No. PB-216188, 1973.
- 18 V. C. Farmer, *The Infrared Spectra of Minerals*, Mineralogical Society, London, 1974.
- 19 A. Rulmont, R. Cahay, M. Liegeois-Duyckaerts and P. Tarte, *Eur. J. Solid State Inorg. Chem.*, 1991, **28**, 207.
- 20 W. H. Bauer, *Acta Crystallogr., Sect. B*, 1974, **30**, 1195.
- 21 U. Schülke and N. N. Chudinova, *Izv. Akad. Nauk SSSR, Neorg. Mater.*, 1974, **10**, 1967.
- 22 O. Y. Miroshnichenko and V. V. Monbelli, *Russ. J. Inorg. Chem., (Engl. Transl.)* 1979, **24**, 1631.
- 23 A. Leclaire, M. M. Borel, A. Grandin and B. Raveau, *J. Solid. State Chem.*, 1989, **78**, 220.
- 24 K. H. Lii, J. J. Chen and S. L. Wang, *J. Solid. State Chem.*, 1989, **78**, 178.
- 25 R. C. Haushalter and F. W. Lai, *J. Solid. State Chem.*, 1988, **76**, 218.
- 26 A. B. P. Lever, *Inorganic Electronic Spectroscopy*, Elsevier, London, 1984.
- 27 R. F. Dallinger and W. H. Woodruff, *J. Am. Chem. Soc.*, 1979, **101**, 4391.
- 28 Y. Sugiura and Y. Hirayama, *J. Am. Chem. Soc.*, 1977, **99**, 1581.
- 29 M. J. Weber, S. A. Brawer and A. J. Degroot, *Phys. Rev. B*, 1981, **23**, 11.
- 30 K. W. Hipps, *Inorg. Chem.*, 1980, **19**, 1930.
- 31 D. Reinen, *Struct. Bonding (Berlin)*, 1969, **6**, 30.
- 32 R. L. Carlin, *Magnetochemistry*, Springer, Berlin, 1986.
- 33 B. A. Averill and W. H. Orme-Johnson, *Inorg. Chem.*, 1980, **19**, 1702.
- 34 E. Pedersen and H. Toftlund, *Inorg. Chem.*, 1974, **13**, 1603.
- 35 F. E. Mabbs and D. Collison, *Electron Paramagnetic Resonance of d Transition Metal Compounds*, Elsevier, Amsterdam, 1992.
- 36 G. S. Rushbrooke and P. J. Wood, *Mol. Phys.*, 1958, **1**, 257.

Paper 7/02733H; Received 22nd April, 1997